



HAL
open science

Concentration and purification by crossflow microfiltration with diafiltration of carotenoids from a by-product of cashew apple juice processing

Adrien Servent, Fernando A.P. Abreu, Claudie Dhuique-Mayer, Marie-Pierre Belleville, Manuel Dornier

► To cite this version:

Adrien Servent, Fernando A.P. Abreu, Claudie Dhuique-Mayer, Marie-Pierre Belleville, Manuel Dornier. Concentration and purification by crossflow microfiltration with diafiltration of carotenoids from a by-product of cashew apple juice processing. *Innovative Food Science & Emerging Technologies / Innovative Food Science and Emerging Technologies*, 2020, 66, pp.102519 -. 10.1016/j.ifset.2020.102519. hal-03492687

HAL Id: hal-03492687

<https://hal.science/hal-03492687>

Submitted on 17 Oct 2022

HAL is a multi-disciplinary open access archive for the deposit and dissemination of scientific research documents, whether they are published or not. The documents may come from teaching and research institutions in France or abroad, or from public or private research centers.

L'archive ouverte pluridisciplinaire **HAL**, est destinée au dépôt et à la diffusion de documents scientifiques de niveau recherche, publiés ou non, émanant des établissements d'enseignement et de recherche français ou étrangers, des laboratoires publics ou privés.



Distributed under a Creative Commons Attribution - NonCommercial 4.0 International License

1 Concentration and purification by crossflow microfiltration with 2 diafiltration of carotenoids from a by-product of cashew apple 3 juice processing

4

5 SERVENT Adrien^{1,2}, ABREU Fernando A. P.³, DHUIQUE-MAYER Claudie^{1,2},
6 BELLEVILLE Marie-Pierre⁴, DORNIER Manuel^{1*}

7

8 ¹ QualiSud, Univ Montpellier, CIRAD, Institut Agro, Univ Avignon, Univ La Réunion,
9 Montpellier, France

10 ² CIRAD, UMR QualiSud, F-34398 Montpellier, France

11 ³ Embrapa Agroindústria Tropical, av. Dra. Sara Mesquita 2270, CEP 60511-110, Planalto
12 Pici, Fortaleza, Ceará, Brazil

13 ⁴ IEM, Univ Montpellier, CNRS, ENSCM, Montpellier, France

14

15 *Corresponding author: manuel.dornier@supagro.fr

16

17 Declarations of interest: none

18

19 Abstract

20 This work aimed to further investigate microfiltration with diafiltration to obtain a rich
21 carotenoid extract from the solid by-product of cashew apple (*Anacardium occidentale* L.)
22 juice processing. This solid residue called cashew fibers is rich in bioactive compounds,
23 especially carotenoids. After mixing with water and pressing, an aqueous suspension was
24 obtained and processed by crossflow microfiltration (40°C) using tubular ceramic membrane
25 with 0.2 µm pore diameter. Permeate flux, which increased with transmembrane pressure,
26 could be maintained above 100 L·h⁻¹·m⁻² at high volume reduction ratio by coupling
27 mechanical extraction with enzyme liquefaction. The concentration step led to an increase of
28 the carotenoid content by up to 19-fold and the diafiltration step allowed the carotenoid purity
29 to be multiplied by 5. The impact of the process on the retentate characteristics was assessed
30 using a model based on simple assumptions. This calculation tool can easily be implemented
31 and is helpful for choosing the operating conditions, to minimize water consumption as well
32 as effluent production.

33

34 Industrial relevance text

35 A driven pressure membrane operation is a mild and economic process which covers a broad
36 variety of applications in the food industry. Most operations focus on permeate (clarification,
37 cold sterilization, etc.), however few attempts have been made to exploit the retentate which is
38 considered as waste in many cases. In this study, we devised an approach for an integrated
39 process of extraction and crossflow filtration combined with enzymatic liquefaction in order
40 to produce a carotenoid-rich extract from cashew apple fibers. This work also provided
41 opportunities for cashew apple juice manufacturers to add value to their by-products at low
42 cost, simultaneously producing a high value-added extract and a ready-to-drink clarified juice.
43 Another originality of this work was to provide a simple equation set, accessible on an
44 industrial scale, to forecast the effluent volume and the consumption of water during
45 diafiltration, by setting a target concentration factor and a target purification factor, correlated
46 to the limit of the purification rate. This work can help industrials to plan production

47 providing them with the possibility of steering the process with a balance between final
48 product quality, process productivity, effluent generation and water consumption.

49 **Highlights**

50 Integrated extraction-filtration process of cashew fibers with enzyme liquefaction
51 Total carotenoid retention during concentration and purification by microfiltration
52 High permeate flux at a volume reduction ratio of up to 20
53 Carotenoid purity multiplied by 5 using diafiltration
54 Modelling to forecast purification rate minimizing effluent volume and water consumption

55
56

57 **Keywords:** microfiltration efficiency, purification rate, diafiltration performance, carotenoid
58 rejection, enzyme liquefaction

59

60 **Abbreviations**

61 α : purification rate (no unit)
62 CF: concentration factor (no unit)
63 C: carotenoid concentration ($\text{mg}\cdot\text{kg}^{-1}$)
64 DM: dry matter ($\text{g}\cdot\text{kg}^{-1}$)
65 DVR: diavolume ratio (no unit)
66 J_p : permeate flux ($\text{L}\cdot\text{h}^{-1}\cdot\text{m}^{-2}$)
67 p: purity of carotenoids ($\text{mg}\cdot\text{kg}^{-1}$)
68 PF: purification factor (no unit)
69 R: retention rate (no unit)
70 SIS: suspended insoluble solids ($\text{g}\cdot\text{kg}^{-1}$)
71 TmP: transmembrane pressure (bar)
72 TSS: total soluble solids ($\text{g}\cdot\text{kg}^{-1}$)
73 VRR: volume reduction ratio (no unit)
74 V: volume (L)

75

76 Subscripts 0, r, p refer to initial, retentate and permeate respectively

77

78 **1. Introduction**

79 Over the last decades, crossflow microfiltration, and more broadly pressure-driven membrane
80 processes, have been further developed for the fruit juice industry for multiple operations
81 including clarification, sterilization, concentration or fractionation (Conidi et al., 2020;
82 Dornier et al., 2018; Lipnizki, 2010). Crossflow microfiltration involves suspensions and is
83 performed to separate insoluble compounds (particles, droplets, colloids) using 0.1 to 10 μm
84 pore diameter membranes while ultra- and nanofiltration are used for solute fractionation over
85 a large molecular weight range. Crossflow microfiltration under 0.2 μm pore diameter is
86 mainly carried out as a unit operation throughout the technology chain in the food industry.
87 This mild process is often used to decrease the particle content in a liquid (clarification), as a
88 pre-treatment to prevent any problems with subsequent operations (chromatographic
89 separation, other membrane processes, etc.), and to lower the microbial load in the permeate
90 (Dornier et al., 2018). For industrial applications, multiple parameters should be considered
91 including environmental, economic or technological ones. Regarding the process, key
92 parameters such as permeate flux, yields and rejections have to be evaluated and optimized to
93 estimate the large-scale feasibility. Microfiltration is often associated with an enzymatic
94 treatment which aims to reduce viscosity and fouling, and in most cases, to improve the
95 system performance (De Oliveira et al., 2012; Laorko et al., 2010; Vaillant et al., 2005). Since
96 the enzymes used are a mix of pectinases, cellulases and hemicellulases from mold cultures
97 which are commonly used in the fruit processing industry, the cost of such processing aids is
98 generally low, compared to the productivity gain. Most studies of membranes carried out in
99 various fields, have generally focused on enhancing the value of permeate while only a few
100 have highlighted retentate potential. For their part, they mainly describe the concentration and
101 the purification of bioactive compounds, associated with the comprehension of fouling
102 mechanisms in complex matrices (Cho et al., 2003; Cisse et al., 2011; Dahdouh et al., 2016).

103 Cashew apple (*Anacardium occidentale L.*) is cultivated on a large scale, especially in Brazil
104 which ranked 1st in 2018 producing more than 1 500 000 tons according to FAO statistics. It
105 is associated with cashew nut production, which is the main reason why it is produced,
106 however it suffers from considerable post-harvest losses (Das & Arora, 2017). It is associated
107 with cashew nut production, which is the main reason why it is produced. It has been reported
108 to be rich in organic acids, sugars, polysaccharides, mostly pectin, and in phytochemicals,
109 such as polyphenols, mainly flavonoids and tannins, carotenoids and vitamins, especially
110 vitamin C. Like all fruits, it is highly perishable, and spoilage of the pulp occurs rapidly, only
111 a few hours after fruit injury or during the first step of juice processing. The type of spoilage
112 observed is usual, namely fermentation and oxidation leading mainly to browning and
113 astringency development (Das & Arora, 2017). Cashew apple that is intended for human
114 consumption, is processed into multiple products such as sweet foods (candies, jam, etc.) or
115 beverages. This industrial production leads to the rejection of waste in significant quantities
116 which is named cashew apple fibers (Damasceno et al., 2008; Talasila & Shaik, 2015). This
117 by-product, mainly destined for animal food production, is however rich in bioactive
118 compounds, especially carotenoids. Carotenoids are liposoluble compounds that have been
119 studied for years because of their role as colorants and antioxidants. In addition to the pro-
120 vitamin A status of some of them, they present known and significant beneficial effects on
121 human health, for instance, reducing the risk of cancer, cardiovascular disease and cellular
122 degeneration (Rao & Rao, 2007). Pinto de Abreu et al. (2013), have characterized the
123 carotenoids and their relative contents in cashew apple fibers. The carotenoids identified were
124 mainly xanthophylls, such as auroxanthin, mutatoxanthin, lutein, zeaxanthin and β -
125 cryptoxanthin at 31, 24.5, 10.4, 11 and 15% of total carotenoids respectively, but also
126 carotenes, mostly β -carotene, at 7.4%. In this work, the authors highlighted an approach using
127 pressing and enzyme treatment in order to optimize the extraction of carotenoids from cashew

128 fibers. A strategy based on a continuous helical-type press was suggested for optimal
129 carotenoid extraction, and a microfiltration trial was mentioned in order to obtain a
130 concentrated extract. Campos et al. (2002) and Castro et al. (2007) presented interesting
131 results using this strategy, demonstrating the feasibility of crossflow microfiltration applied to
132 cashew apple juice to decrease the microflora in the clarified permeate.

133 Crossflow microfiltration coupled with enzyme liquefaction, resulted in two promising
134 derived products with significant process performance. In the case of melon juice, Vaillant et
135 al. (2005) obtained on one hand a retentate enriched 4-fold in β -carotene, and on the other a
136 clarified permeate which was organoleptically close to fresh melon juice. Introducing a
137 diafiltration step allows the purity of the obtained fractions to be increased. For watermelon,
138 integrated processes combining crossflow microfiltration and enzyme liquefaction have been
139 developed for the production of a bioactive lycopene extract, concentrated between 8 and 11-
140 fold and purified up to 25-fold by diafiltration (Chaparro et al., 2016) or between 12 and 18-
141 fold, resulting in a higher antioxidant capacity of the extract (Oliveira et al., 2016). Using *in*
142 *vitro* human digestion models, Gence et al. (2018) highlighted the nutritional interest of a
143 clementine juice concentrated 8-fold by crossflow microfiltration, taking into account
144 carotenoid bioaccessibility. This research also underlined the benefit of considering the
145 retentate as a high-value product, both economically and nutritionally.

146 Recently, a study was performed in order to assess the feasibility of coupling crossflow
147 microfiltration and diafiltration for carotenoid concentration and purification from orange
148 juice using an industrial approach (Polidori et al., 2018). In addition to the production of a
149 concentrated carotenoid extract between 5 and 10-fold which was purified over a range of 8 to
150 20-fold by diafiltration with relevant process performances, the authors provided and
151 validated a model based on simple assumptions in order to predict concentration and
152 purification factors according to targeted conditions or *vice versa* on any filtration scale.

153 The present work aims to study the microfiltration process that includes a diafiltration step for
154 concentration and purification of carotenoids in an aqueous extract obtained from cashew
155 apple fibers. It includes an evaluation of the interest of coupling the process with enzymatic
156 liquefaction. The study proposes to address the operation integrating product quality, process
157 productivity, and part of the environmental impact. A special focus is placed on developing a
158 simple simulation tool for helping the user to choose operating conditions that result in the
159 targeted concentration and purification levels minimizing effluent generation and processing
160 duration.

161

162 **2. Experimental**

163 **2.1 Cashew juice material**

164 Raw material obtained from the by-product of cashew apple juice production as described by
165 Pinto de Abreu et al. (2013), was supplied by Sabor Tropical Ltda (Ceará, Brazil) and was
166 produced from the CCP-076 variety of cashew apple developed by Embrapa. This by-product,
167 called cashew apple fibers, was mixed with water using a mass ratio of 1:1. At this stage,
168 maceration for 60 min at 55°C with 500 mg·kg⁻¹ of pectinolytic enzyme Ultrazym AFP-L
169 (Novozymes, Bagsvaerd, Denmark) was, in certain cases, carried out. This aimed to improve
170 the release of carotenoids that are strongly entrapped within cell structures. The resulting
171 mixture was then pressed in a helical-type press with a nominal capacity of 300 kg·h⁻¹ using a
172 rotational speed of 30 rpm (Incomat 300, Fortaleza, Brazil). This operation was repeated 6
173 times after remixing the two phases obtained. The final extract was filtered through a 0.3 mm
174 sieve. For the study, one homogeneous batch of around 230 L of final extract was constituted,
175 distributed in sealed 3-10 L polyethylene bags and frozen at -20°C until use.

176 **2.2 Microfiltration process: clarification & purification**

177 Microfiltration trials were carried out at laboratory scale using a micro-pilot manufactured by
178 TIA (Bollène, France). This device is described in figure 1. It consisted of 4 single-channel
179 tubular α -alumina membranes of 55 cm² each, with an average pore diameter of 0.2 μ m,
180 mounted in series (Pall Exekia, Bazet, France). This configuration allowed the simultaneous
181 testing of 4 transmembrane pressure (TmP) conditions ranging from 1.2 to 3.2 bar. For each
182 membrane TmP was evaluated from the input and output pressures in the retentate loop
183 considering head losses as linear. Crossflow velocity was set at around 6 m·s⁻¹ independently
184 of TmP using a volumetric feed pump. This high value ensured that the system acted as a
185 perfectly stirred reactor. The temperature of the whole system was maintained at 40 \pm 2°C
186 using a heat exchanger connected to a running water cryostat. This pilot was equipped with a
187 feeding tank of 3 L. Membrane cleaning operations were based on manufacturer
188 recommendations, including classical alkaline (NaOH 2 %, 80°C, 20 min without pressure, 20
189 min with pressure) and acidic phases (HNO₃ 1 %, 50°C, 20 min), and was controlled by the
190 verification of pure water permeability (374 \pm 103 L·h⁻¹·m⁻²·bar⁻¹ at 25°C and 6 m·s⁻¹).

191 As usual, the concentration level of the extract was characterized by the volume reduction
192 ratio (VRR) defined according to the volumes of permeate V_p and retentate V_r (Equation 1).

193
$$VRR = \frac{V_r + V_p}{V_r} = 1 + \frac{V_p}{V_r} \quad (1)$$

194 Each filtration was carried out in concentration mode extracting the permeate continuously.
195 Starting with 2.5-3 L of the product, the system was continuously fed with fresh raw extract,
196 maintaining the retentate volume constant (concentration at constant volume) up to VRR
197 between 5 and 8. Then, in order to reach a higher VRR more quickly, feeding was stopped,
198 allowing the volume of the retentate to decrease (concentration at variable volume). At the
199 end of the concentration step, the V_r was still 1.5 L. During filtration, the retention rate (R) is

200 defined using Equation 2 comparing the concentrations in the permeate (C_p) and in the
201 retentate (C_r) as usual.

$$202 \quad R = 1 - \frac{C_p}{C_r} \quad (2)$$

203 A diafiltration step could then be added at the end of the concentration step when the targeted
204 VRR was reached. In this case, diafiltration was carried out at constant V_r value (1.5 L) by
205 feeding the system with distilled water instead of fresh raw extract in order to compensate the
206 volume of permeate recovered. Therefore, the diafiltration was continuous, without
207 interruption between the concentration and the diafiltration steps. This diafiltration mode
208 allowed water consumption to be minimized because it was carried out at the end of the
209 concentration step when V_r was the lowest (Polidori et al. 2018). Diafiltration ended when
210 permeate reached a content of total soluble solids below $5 \text{ g}\cdot\text{kg}^{-1}$. The diavolume ratio (DVR)
211 was defined as the ratio between the volume of added water V_w and V_r (Equation 3). It can
212 also be considered as a water consumption indicator.

$$213 \quad DVR = \frac{V_w}{V_r} \quad (3)$$

214 **2.3 Extract analysis**

215 Total soluble solids (TSS) were measured with a PAL- α refractometer (Atago, Tokyo, Japan)
216 with $\pm 0.5 \text{ g}\cdot\text{kg}^{-1}$ of bias. To assess the suspended soluble solids (SIS), a sample of precisely
217 20 g was homogenized and centrifuged at $14\,000 \times g$ for 20 min (Allegra 21 centrifuge,
218 Beckman Coulter, USA). The supernatant was discarded and replaced by 20 g of deionized
219 water and then the sample was homogenized and centrifuged again. After 3 repetitions, the
220 residue was dried at 70°C under vacuum (100 mPa) and weighted. The term dry matter (DM)
221 refers to the residues remaining after the total evaporation of water. DM includes both TSS
222 and SIS. Therefore, it was calculated as the sum of these two fractions.

223 To quantify the total carotenoid content, 10 mL of the sample to be analyzed were
224 homogenized with 35 mL of a mixture made of ethanol/hexane (4:3 v/v) (Sigma-Aldrich,
225 Santa-Clara, USA). After dephasing in a separating funnel, the organic phase was recovered,
226 dried with anhydrous sodium sulfate (Sigma-Aldrich, Santa Clara, USA) and its absorbance
227 was then measured at 450 nm with a Variant 50 Bio spectrophotometer (Variant Inc,
228 California, USA). Results were expressed in mg β -carotene equivalent using the molar
229 extinction coefficient of β -carotene at 450 nm. Carotenoid purity p was calculated as
230 carotenoid content expressed in DM.

231 All analyses were carried out in triplicates.

232 **2.4 Modelling**

233 Assuming that there were no losses of matter during the operation, that the system behaved
234 like a perfectly stirred reactor and that the retentions were constant, the retentate composition
235 could be predicted using a simple equation set tested in previous studies (Acosta et al., 2014;
236 Polidori et al., 2018). Indeed, since the insoluble compounds (SIS and carotenoids) were
237 completely retained by the membrane, unlike the TSS, which were not retained at all
238 (Chaparro et al., 2016; Oliveira et al., 2016; Polidori et al., 2018), carotenoid concentration
239 (C), SIS and TSS could be calculated in the final retentate from volume reduction ratio
240 (VRR), diavolume ratio (DVR) and initial values (subscript 0) using Equations 4 to 6.

$$241 \quad C = C_0 VRR \quad (4)$$

$$242 \quad SIS = SIS_0 VRR \quad (5)$$

$$243 \quad TSS = TSS_0 e^{-DVR} \quad (6)$$

244 Therefore, for carotenoids the concentration factor in the retentate (CF) is equal to the VRR.

245 Since DM is the sum of SIS and TSS, the purity of carotenoids in the retentate p and the
246 purification factor (PF) could be assessed through Equations 7 and 8.

$$247 \quad p = \frac{C_0 VRR}{SIS_0 VRR + TSS_0 e^{-DVR}} \quad (7)$$

$$248 \quad PF = \frac{(SIS_0 + TSS_0) VRR}{SIS_0 VRR + TSS_0 e^{-DVR}} \quad (8)$$

249 In this case, the purity of carotenoids cannot exceed the ratio C_0/SIS_0 when DVR increases.
250 Thus, whatever the VRR, it is not possible to exceed a maximum purification factor PF_{lim} . In
251 order to quantify the progress of the purification, we defined the ratio between the obtained
252 PF and PF_{lim} (Equation 9). It ranges from 0 to 1 and was called the purification rate α
253 (Equation 10).

$$254 \quad PF = \alpha PF_{lim} = \alpha (TSS_0/SIS_0 + 1) \quad (9)$$

$$255 \quad \alpha = \frac{VRR}{VRR + (TSS_0/SIS_0) e^{-DVR}} \quad (10)$$

256

257 **3. Results and discussions**

258 **3.1. Effect of transmembrane pressure**

259 In order to find an optimal transmembrane pressure, preliminary trials were carried out using
260 the extract obtained without enzymes (Table 1) up to a VRR of around 10. In figure 2, the
261 permeate flux (J_p) during microfiltration of cashew apple extract without enzyme liquefaction
262 using 5 growing TmP (from 2.2 to 3.2 bar) were plotted versus VRR. As presented, permeate
263 flux abruptly decreased at the beginning as soon as concentration occurred. This initial phase
264 is usual in crossflow microfiltration and corresponds to a rapid membrane fouling mainly due
265 to accumulation of insoluble solids on the membrane surface (external fouling) and/or into the
266 membrane pores (internal fouling). This fouling leads to an increase in the total hydraulic

267 resistance of the system and so causes the drop in transmembrane flux. Shortly afterwards,
268 from a VRR of around 1.2, the flux decrease slowed down, what could be linked to back-
269 transport phenomena due to crossflow velocity that counterbalanced the input of fouling
270 material to the membrane. From a VRR = 3, J_p stabilized up to the final VRR. This behavior
271 was observed irrespective of the transmembrane pressure. By comparison with many
272 references in literature that dealt with crossflow microfiltration of various fruit juices, these
273 last results were different (Emani et al., 2013; Fukumoto et al., 1998; Qin et al., 2015;
274 Ushikubo et al., 2007; Wang et al., 2005). Even if the flux range was in accordance with the
275 values generally mentioned for fruit juice microfiltration (Dornier et al., 2018; Rai & De,
276 2009), stabilization at such a high VRR is uncommon. Generally transmembrane transfers are
277 continuously slowed down by the increase in viscosity and fouling power of the retentate
278 during concentration (Tarabara et al., 2002). This original behavior was probably linked to the
279 extract composition that was quite different from classical fruit juices in terms of
280 soluble/colloidal/insoluble fractions and led to a more moderate fouling of the membrane
281 during concentration. Indeed, it is well established that fouling not only depends on the
282 hydrodynamic conditions in the vicinity of the membrane but also on suspension
283 characteristics (Dahdouh et al., 2016). Nevertheless, because the phenomena involved in
284 membrane fouling are multiple and complex, further investigations should be carried out for a
285 better understanding. This configuration is particularly favorable for an industrial application
286 as it makes it possible to reconcile high concentration factors and high treatment processing
287 rates, close to $100 \text{ L}\cdot\text{h}^{-1}\cdot\text{m}^{-2}$, considered very interesting from an economic point of view for
288 microfiltration of food liquids (Daufin et al., 2001). This promising performance underlined
289 the fact that the fouling property of the product was limited.

290 The figure 3 represented the stabilized permeate flux J_p depending on the used TmP (from 2.2
291 to 3.2 bar) for a range of VRR between 1 to 9. Comparing the permeate flux for the same

292 VRR, it linearly increased with pressure both at low and high VRR. These results showed that
293 permeate fluxes were mainly impacted by the driving force of the mass transfer through the
294 porous medium (i.e. the transmembrane pressure gradient) with a total hydraulic resistance of
295 the system, defined according to the generalized Darcy's law, that increased with the
296 volumetric reduction level at low VRR and then tended to a constant value for higher VRR.
297 Therefore, in the chosen operating conditions, high TmP at about 3 bar has to be selected in
298 order to maximize permeate flux whatever the desired targeted concentration factor for
299 carotenoids. These experimental results were significantly different from those obtained by
300 Polidori et al. (2018) with orange juice which showed that the effect of pressure on permeate
301 flux depended on VRR. The much weaker fouling power of cashew apple fiber extract could
302 be linked, as mentioned by Dahdouh et al., (2016); Vaillant et al., (2008) and Tarabara et al.,
303 (2002), to multiple factors such as its composition, particle size distribution and rheological
304 characteristics, related to the specific extraction press-processing, but further studies are
305 needed to confirm this.

306 **3.2. Effect of enzymatic liquefaction during extraction**

307 Extracts obtained with and without enzyme treatment exhibited very similar TSS and SIS
308 contents (Table 1). Thus, liquefaction did not drastically modify the soluble/insoluble solid
309 distribution in the final product. On the contrary, carotenoid content was 30% higher in the
310 enzyme-treated product, which confirmed the enzyme liquefaction enhanced extractable
311 fraction of carotenoids. This observation is probably due to cell wall weakening leading to the
312 depolymerization of pectin chains through polygalacturonase and pectin-lyase activities
313 (Çinar, 2005). It favored cell breakdown during the pressing and so allowed a better release of
314 carotenoids. This higher recovery of phytochemicals using enzymes is consistent with various
315 other studies (Acosta et al., 2014; Carneiro et al., 2002; Çinar, 2005; Puri et al., 2012).

316 Both these extracts then underwent microfiltration up to a VRR of about 20 using high
317 transmembrane pressure (Figure 4). First, repetitions showed that the process was repeatable
318 with a difference of permeate flux for the same operating conditions of around 10%, which is
319 similar to the repeatability usually achieved using a crossflow microfiltration pilot unit at
320 laboratory scale. Second, the interest of the liquefaction as a pre-treatment is clearly
321 demonstrated from the point of view of process performance. Indeed, combining enzyme
322 liquefaction with physical treatment resulted in the permeate flux being multiplied by 1.5. For
323 the extract with enzyme liquefaction, after a first drop of up to VRR=3, the permeate flux
324 stopped decreasing and remained at around $140 \text{ L}\cdot\text{h}^{-1}\cdot\text{m}^{-2}$ up to VRR=19. Therefore, the
325 extraction procedure resulted in a multiphasic solution being obtained, in which high fouling
326 compounds were removed. This positive effect of enzyme liquefaction on the filterability has
327 already been well illustrated in many cases with fruit juices (Domingues et al., 2014;
328 Machado et al., 2012; Pinelo et al., 2010; Rai et al., 2007). It is not only related to the
329 viscosity decrease of the product due to depolymerization and demethylation of the soluble
330 pectic compounds, but probably also to changes of the fouling power of the insoluble fraction
331 (Dahdouh et al., 2016; Vaillant et al., 2008). These insoluble solids mainly consist of tissue
332 and cell fragments that can be greatly modified by pectinolytic and cellulolytic enzymes
333 through the deconstruction of cell walls. Therefore, the interest of the enzymatic treatment
334 was twofold: it led not only to an increase in the carotenoid extraction yield but also to a
335 significant improvement in the performance of the subsequent operation of separation.
336 Because the chosen enzymes were classical adjuvants commonly used in fruit juice industry,
337 they were not purified and consequently were not very expensive. So as often in fruit juice
338 processing, the additional cost of using enzymes would probably be justified by the reduction
339 in investment (membrane area needed) and operating costs (time, energy).

340 These first trials also confirmed that in all the cases, with or without enzyme liquefaction,
341 carotenoids and SIS were completely retained by the membrane (neither carotenoid nor SIS
342 were found in the permeate, $R = 1$) and that there was no solute retention (same TSS content
343 in permeate and retentate, $R = 0$).

344 **3.3. Purification by diafiltration**

345 To improve the purity of the carotenoids, a diafiltration step was added to the concentration
346 process. Diafiltration is simple to carry out, but for industrial application a compromise
347 between permeate flux and water consumption has to be found (Fikar et al., 2010). Indeed, for
348 a targeted purification rate, if the diafiltration is implemented at the beginning of the
349 concentration step, i.e. at low VRR, the permeate flux will be at a very good level but the
350 volume of water needed will be substantial. On the contrary, the higher the VRR chosen for
351 diafiltration, the worse the flux might be, but at the same time, the amount of water needed
352 will be lower. In the case of cashew apple extract, because permeate fluxes were maintained
353 at a high value at high VRR, it was clear that priority had to be given to water savings. For
354 that reason, we chose to conduct diafiltration at the end of the concentration phase. When the
355 retentate volume reached the minimal operational volume in the system, and therefore
356 targeted VRR was achieved, cashew apple extract was replaced by water to feed the device
357 and diafiltration began.

358 Figure 5 represents the evolution of DVR, VRR, TSS and J_p as a function of time during the
359 process that included diafiltration. The first part of the filtration referred to a regular VRR
360 increase of up to 6-7. During this phase, the volume of retentate was maintained constant by
361 compensating the volume of permeate removed through feeding the system with the same
362 volume of cashew apple extract. Afterwards, a rapid increase of VRR was observed as the
363 feed was stopped in a second phase and thus the volume of the retentate circulating in the
364 concentration loop rapidly decreased. Once the VRR setpoint was reached, diafiltration was

365 initiated compensating the volume of extracted permeate by the same volume of water and so
366 DVR increased. It is worth noting that after the initial drop, permeate fluxes remained almost
367 constant throughout the concentration and diafiltration steps. Only a slight increase was
368 observed during the diafiltration step, due to the diminution of viscosity caused by dilution
369 with water. In addition, the values obtained were very similar to those obtained previously.
370 From around $230 \text{ L}\cdot\text{h}^{-1}\cdot\text{m}^{-2}$ at the beginning, they stabilized at $\text{VRR}=19$ at about $130 \text{ L}\cdot\text{h}^{-1}\cdot\text{m}^{-2}$
371 and $75 \text{ L}\cdot\text{h}^{-1}\cdot\text{m}^{-2}$ for enzyme liquefied and untreated extracts respectively. By using
372 enzymes, the time needed to reach $\text{VRR}=19$ was 30% shorter and the time needed to reach a
373 DVR of 3.5, was reduced by 40%. As expected, TSS decreased exponentially in the system as
374 soon as the diafiltration step started. This also implied that the system could be considered as
375 being very similar to a perfectly stirred reactor. Obviously, the time needed to reach a TSS
376 below $5 \text{ g}\cdot\text{kg}^{-1}$ was much shorter for the enzyme treated extract because of the greater
377 permeate flux.

378 Characterization results highlighted that both concentrates exhibited close values considering
379 biochemical analyses (Table 2). TSS decreased considerably following diafiltration. Between
380 92-96% of solutes were removed from the retentate. While for the insoluble fraction (SIS), it
381 was concentrated 18 to 19-fold in accordance with the final VRR. Total carotenoid content
382 was logically higher for enzyme-treated retentate because of the difference between initial
383 contents and of the higher VRR reached. The ratio between the concentration factor CF and
384 VRR was about 1.04 and 1.01 with and without enzymes respectively. Therefore,
385 concentration factors for carotenoids were almost equal to the VRR with and without enzyme
386 liquefaction after diafiltration, as expected. This result showed that there was no loss in
387 carotenoids during processing. It is concomitant with Polidori et al. (2018) who demonstrated
388 similar carotenoid behavior during orange juice microfiltration, using a $0.2 \mu\text{m}$ membrane
389 with a CF/VRR ratio of 1.06 with or without diafiltration. Chaparro et al. (2016) and Oliveira

390 et al. (2016), who studied lycopene concentration from watermelon juice, found a ratio of
391 between 1.00 and 1.06, confirming complete retention of carotenoids. For cashew apple fiber
392 extracts, with or without enzyme liquefaction, the process resulted in a significant
393 improvement of the purity of carotenoids with respect to the total dry matter reaching a
394 purification factor of around 5.

395 **3.4. Modelling**

396 From the initial characteristics of the extract (TSS_0 , SIS_0 , C_0) and assuming that
397 SIS /carotenoid (insoluble fraction) and the TSS (soluble fraction) retentions were respectively
398 equal to 1 and zero, theoretical final values for all characteristics could be evaluated
399 combining equations 4 to 8 for the targeted VRR and DVR values. In all the cases, the
400 predicted compositions of the final retentate were very close to the experimental values (Table
401 2). A slight deviation can be noticed for TSS , probably because the hypothesis of a perfectly
402 stirred reactor was not entirely true. Nevertheless, these results validated the model with its
403 assumptions. Thanks to a simple set of calculations, it is thus possible to predict the quality of
404 the extract or to simulate situations without carrying out extensive experiments. Therefore, the
405 question of purification rate can be put forward in order to better optimize the diafiltration
406 step. At VRR of 18-19 with DVR of 3-4, the reached purification rates α were close to the
407 maximum, over 0.99. Obviously, the maximum purity that can be achieved with the process is
408 indeed reached. However, through calculation, we showed that a DVR of 1.5 (that
409 corresponds to a final TSS of 11-12 $g \cdot kg^{-1}$) would be sufficient to reach a α of 0.95, which is
410 already a very interesting value. Therefore, the maximum purity that is achievable can be
411 reasonably attained at lower DVR (1.5 instead of 4), allowing water consumption to be more
412 than halved, to reduce processing time by around 20% and to decrease the production of
413 permeate, considered here as an effluent to be treated, by 10%.

414 This model can be easily generalized for all the VRR/DVR combinations. For example, it can
415 be used to generate charts that link DVR and α as a function of the chosen concentration
416 factor (Figures 6 and 7). These couples of figures are presented for two different TSS₀/SIS₀
417 ratios. The first one corresponds to cashew apple fiber extract with a ratio of 4, and the second
418 one corresponds to a classical fruit juice with a ratio of 33. These charts could be useful to
419 quickly determine the DVR to be used for given concentration level and purification rate. We
420 can notice in the equation set how important the TSS₀/SIS₀ rate is. The higher this quotient
421 and the lower the concentration factor to be reached, the higher the DVR needed to obtain a
422 targeted purification level. Applied to our extract that had a TSS₀/SIS₀ value of 4 plotted in
423 figure 6 or to a citrus fruit juice with a TSS₀/SIS₀ ratio of 33 for instance illustrated in figure 7
424 (Polidori et al., 2018), the obtained curve pattern is completely different.

425 For industrial applications a compromise should often be found between permeate flux,
426 concentration factor, purification rate and water consumption. In this respect, the tested model
427 is an interesting tool that should help for the guidance of the process considering the
428 functional potential of the carotenoid concentrate and, the economic cost of the operation.

429 **4. Conclusion**

430 The aim of this work was to evaluate crossflow microfiltration in order to produce a
431 concentrate that is enriched and purified in carotenoids from the extract of a cashew apple by-
432 product. The process coupled with enzyme liquefaction and using a transmembrane pressure
433 around 3 bar, allowed the carotenoid content to be multiplied by up to 19 while keeping the
434 permeate flux above 100 L·h⁻¹·m⁻². In the case of cashew apple fiber extract, this step
435 complies with the reduction of the energy costs which might render the expense of purchasing
436 the enzyme negligible when compared to the increase in volume production. Adding a
437 diafiltration step led to a 5-fold purification of the carotenoids. The final concentrate
438 contained between 0.2 and 0.3 g·kg⁻¹ of carotenoids in dry matter. A simple model was

439 validated that predicted carotenoid concentration and purity according to the filtration
440 conditions, that is to say the VRR and DVR. This model can be used as a decision aid tool for
441 piloting the process in relation to quality, economic and environmental considerations. This
442 study also showed that cashew apples fibers, that are a low-cost and abundant by-product
443 from the fruit juice industry, especially in Brazil, could be easily treated in order to obtain
444 interesting carotenoid concentrates through the described process. The final extract can be
445 directly used as a natural food coloring and provides an important added value. So, crossflow
446 microfiltration can find its place in sustainable development for the cashew apple processing
447 chain. However, to consider any industrial application, further studies must be conducted on a
448 larger scale, with higher membrane area in order to validate the robustness of the process.
449 Moreover, other aspects such as environmental impact and economic criteria (investment and
450 operation costs) have to be considered in order to demonstrate the interest of an industrial line
451 establishment and scale up, according to the targeted production capacity, equipment
452 availability and local constraints. Eventually, the compositional characterization of the extract
453 has to be completed in order to better evaluate its potential but also to better understand the
454 impact of the process on its composition. The stability of the extract during storage should be
455 investigated in order to determine its shelf life as well.

456

457 **Acknowledgements & Funding**

458 This work was part of the “Producing added value from under-utilized tropical fruit crops
459 with high commercial potential” project (PAVUC) from the FP6-INCO program of the
460 European Commission. The authors express thanks to Embrapa (Agrofuturo program) and
461 Cirad (Persyst dept.) for their financial contributions. Finally, special acknowledgements to
462 Dr. Lourdes Maria Corrêa Cabral from Embrapa Agroindústria de Alimentos (Rio de Janeiro)
463 for her unfailing support in this project.

464

465 **REFERENCES**

- 466 Acosta, O., Vaillant, F., Pérez, A. M., & Dornier, M. (2014). Potential of ultrafiltration for separation
467 and purification of ellagitannins in blackberry (*Rubus adenotrichus* Schltdl.) juice. *Separation*
468 *and Purification Technology*, 125, 120–125.
469 <https://doi.org/https://doi.org/10.1016/j.seppur.2014.01.037>
- 470 Campos, D. C. P., Santos, A. S., Wolkoff, D. B., Matta, V. M., Cabral, L. M. C., & Couri, S. (2002).
471 Cashew apple juice stabilization by microfiltration. *Desalination*, 148(1), 61–65.
472 [https://doi.org/https://doi.org/10.1016/S0011-9164\(02\)00654-9](https://doi.org/https://doi.org/10.1016/S0011-9164(02)00654-9)
- 473 Carneiro, L., dos Santos Sa, I., dos Santos Gomes, F., Matta, V. M., & Cabral, L. M. C. (2002). Cold
474 sterilization and clarification of pineapple juice by tangential microfiltration. *Desalination*,
475 148(1), 93–98. [https://doi.org/https://doi.org/10.1016/S0011-9164\(02\)00659-8](https://doi.org/https://doi.org/10.1016/S0011-9164(02)00659-8)
- 476 Chaparro, L., Dhuique-Mayer, C., Castillo, S., Vaillant, F., Servent, A., & Dornier, M. (2016).
477 Concentration and purification of lycopene from watermelon juice by integrated microfiltration-
478 based processes. *Innovative Food Science & Emerging Technologies*, 37, 153–160.
479 <https://doi.org/https://doi.org/10.1016/j.ifset.2016.08.001>
- 480 Cho, C.-W., Lee, D.-Y., & Kim, C.-W. (2003). Concentration and purification of soluble pectin from
481 mandarin peels using crossflow microfiltration system. *Carbohydrate Polymers*, 54(1), 21–26.
482 [https://doi.org/https://doi.org/10.1016/S0144-8617\(03\)00133-4](https://doi.org/https://doi.org/10.1016/S0144-8617(03)00133-4)
- 483 Çinar, İ. (2005). Effects of cellulase and pectinase concentrations on the colour yield of enzyme
484 extracted plant carotenoids. *Process Biochemistry*, 40(2), 945–949.
485 <https://doi.org/https://doi.org/10.1016/j.procbio.2004.02.022>
- 486 Cisse, M., Vaillant, F., Soro, D., Reynes, M., & Dornier, M. (2011). Crossflow microfiltration for the
487 cold stabilization of roselle (*Hibiscus sabdariffa* L.) extract. *Journal of Food Engineering*, 106(1),
488 20–27. <https://doi.org/https://doi.org/10.1016/j.jfoodeng.2011.04.001>
- 489 Conidi, C., Castro-Muñoz, R., & Cassano, A. (2020). Membrane-Based Operations in the Fruit Juice
490 Processing Industry: A Review. In *Beverages* (Vol. 6, Issue 1, p. 18).
491 <https://doi.org/10.3390/beverages6010018>
- 492 Dahdouh, L., Delalonde, M., Ricci, J., Servent, A., Dornier, M., & Wisniewski, C. (2016). Size-
493 cartography of orange juices foulant particles: Contribution to a better control of fouling during
494 microfiltration. *Journal of Membrane Science*, 509, 164–172.
495 <https://doi.org/https://doi.org/10.1016/j.memsci.2016.01.052>
- 496 Damasceno, L. F., Fernandes, F. A. N., Magalhães, M. M. A., & Brito, E. S. (2008). Non-enzymatic
497 browning in clarified cashew apple juice during thermal treatment: Kinetics and process control.
498 *Food Chemistry*, 106(1), 172–179.
499 <https://doi.org/https://doi.org/10.1016/j.foodchem.2007.05.063>
- 500 Das, I., & Arora, A. (2017). Post-harvest processing technology for cashew apple – A review. *Journal*
501 *of Food Engineering*, 194, 87–98.
502 <https://doi.org/https://doi.org/10.1016/j.jfoodeng.2016.09.011>
- 503 Daufin, G., Escudier, J.-P., Carrère, H., Bérot, S., Fillaudeau, L., & Decloux, M. (2001). Recent and
504 Emerging Applications of Membrane Processes in the Food and Dairy Industry. *Food and*
505 *Bioproducts Processing*, 79(2), 89–102.
506 <https://doi.org/https://doi.org/10.1205/096030801750286131>

- 507 De Castro, T. R., Pinto de Abreu, F., & Beserra Carioca, J. O. (2007). Using membrane separation
508 processes to obtain clarified cashew apple juice. In *Revista Ciencia Agronomica (Brazil): Vol. v.*
509 *38*.
- 510 De Oliveira, R. C., Docê, R. C., & De Barros, S. T. D. (2012). Clarification of passion fruit juice by
511 microfiltration: Analyses of operating parameters, study of membrane fouling and juice quality.
512 *Journal of Food Engineering*, *111*(2), 432–439.
513 <https://doi.org/https://doi.org/10.1016/j.jfoodeng.2012.01.021>
- 514 Domingues, R. C. C., Ramos, A. A., Cardoso, V. L., & Reis, M. H. M. (2014). Microfiltration of passion
515 fruit juice using hollow fibre membranes and evaluation of fouling mechanisms. *Journal of Food*
516 *Engineering*, *121*, 73–79. <https://doi.org/https://doi.org/10.1016/j.jfoodeng.2013.07.037>
- 517 Dornier, M., Belleville, M. P., & Vaillant, F. (2018). Membrane Technologies for Fruit Juice Processing.
518 In *Fruit preservation* (Food Engin). Springer. https://doi.org/10.1007/978-1-4939-3311-2_8
- 519 Emani, S., Uppaluri, R., & Purkait, M. K. (2013). Preparation and characterization of low cost ceramic
520 membranes for mosambi juice clarification. *Desalination*, *317*, 32–40.
521 <https://doi.org/https://doi.org/10.1016/j.desal.2013.02.024>
- 522 Fikar, M., Kovács, Z., & Czermak, P. (2010). Dynamic optimization of batch diafiltration processes.
523 *Journal of Membrane Science*, *355*(1), 168–174.
524 <https://doi.org/https://doi.org/10.1016/j.memsci.2010.03.019>
- 525 Fukumoto, L. R., Delaquis, P., & Girard, B. (1998). Microfiltration and Ultrafiltration Ceramic
526 Membranes for Apple Juice Clarification. *Journal of Food Science*, *63*(5), 845–850.
527 <https://doi.org/10.1111/j.1365-2621.1998.tb17912.x>
- 528 Gence, L., Servent, A., Pouchet, P., Hiol, A., & Dhuique-Mayer, C. (2018). Pectin structure and
529 particle size modify carotenoid bioaccessibility and uptake by Caco-2 cells in citrus juices vs.
530 concentrates. *Food Funct.*, *9*(6), 3523–3531. <https://doi.org/10.1039/C8FO00111A>
- 531 Laorko, A., Li, Z., Tongchitpakdee, S., Chantachum, S., & Youravong, W. (2010). Effect of membrane
532 property and operating conditions on phytochemical properties and permeate flux during
533 clarification of pineapple juice. *Journal of Food Engineering*, *100*(3), 514–521.
534 <https://doi.org/https://doi.org/10.1016/j.jfoodeng.2010.04.039>
- 535 Lipnizki, F. (2010). Cross-Flow Membrane Applications in the Food Industry. In *Membrane Technology*
536 (pp. 1–24). <https://doi.org/doi:10.1002/9783527631384.ch1>
- 537 Machado, R. M. D., Haneda, R. N., Trevisan, B. P., & Fontes, S. R. (2012). Effect of enzymatic
538 treatment on the cross-flow microfiltration of açaí pulp: Analysis of the fouling and recovery of
539 phytochemicals. *Journal of Food Engineering*, *113*(3), 442–452.
540 <https://doi.org/https://doi.org/10.1016/j.jfoodeng.2012.06.022>
- 541 Oliveira, C., Gomes, F., Constant, L., Silva, L., Godoy, R., Tonon, R., & Cabral, L. M. C. (2016).
542 Integrated membrane separation processes aiming to concentrate and purify lycopene from
543 watermelon juice. *Innovative Food Science & Emerging Technologies*, *38*, 149–154.
544 <https://doi.org/https://doi.org/10.1016/j.ifset.2016.09.025>
- 545 Pinelo, M., Zeuner, B., & Meyer, A. S. (2010). Juice clarification by protease and pectinase treatments
546 indicates new roles of pectin and protein in cherry juice turbidity. *Food and Bioprocess*
547 *Processing*, *88*(2), 259–265. <https://doi.org/https://doi.org/10.1016/j.fbp.2009.03.005>
- 548 Pinto De Abreu, F., Dornier, M., Dionisio, A. P., Carail, M., Caris-Veyrat, C., & Dhuique-Mayer, C.

- 549 (2013). Cashew apple (*Anacardium occidentale* L.) extract from by-product of juice processing:
550 A focus on carotenoids. *Food Chemistry*, 138(1), 25–31.
551 <https://doi.org/https://doi.org/10.1016/j.foodchem.2012.10.028>
- 552 Polidori, J., Dhuique-Mayer, C., & Dornier, M. (2018). Crossflow microfiltration coupled with
553 diafiltration to concentrate and purify carotenoids and flavonoids from citrus juices. *Innovative*
554 *Food Science & Emerging Technologies*, 45, 320–329.
555 <https://doi.org/https://doi.org/10.1016/j.ifset.2017.11.015>
- 556 Puri, M., Sharma, D., & Barrow, C. J. (2012). Enzyme-assisted extraction of bioactives from plants.
557 *Trends in Biotechnology*, 30(1), 37–44.
558 <https://doi.org/https://doi.org/10.1016/j.tibtech.2011.06.014>
- 559 Qin, G., Lü, X., Wei, W., Li, J., Cui, R., & Hu, S. (2015). Microfiltration of kiwifruit juice and fouling
560 mechanism using fly-ash-based ceramic membranes. *Food and Bioprocess Processing*, 96, 278–
561 284. <https://doi.org/https://doi.org/10.1016/j.fbp.2015.09.006>
- 562 Rai, P., & De, S. (2009). Clarification of pectin-containing juice using ultrafiltration. *Current Science*,
563 96(10), 1361–1371. <http://www.jstor.org/stable/24105375>
- 564 Rai, P., Majumdar, G. C., Das Gupta, S., & De, S. (2007). Effect of various pretreatment methods on
565 permeate flux and quality during ultrafiltration of mosambi juice. *Journal of Food Engineering*,
566 78(2), 561–568. <https://doi.org/https://doi.org/10.1016/j.jfoodeng.2005.10.024>
- 567 Rao, A. V., & Rao, L. G. (2007). Carotenoids and human health. *Pharmacological Research*, 55(3), 207–
568 216. <https://doi.org/https://doi.org/10.1016/j.phrs.2007.01.012>
- 569 Talasila, U., & Shaik, K. B. (2015). Quality, spoilage and preservation of cashew apple juice: A review.
570 *Journal of Food Science and Technology*, 52(1), 54–62. [https://doi.org/10.1007/s13197-013-](https://doi.org/10.1007/s13197-013-0931-0)
571 0931-0
- 572 Tarabara, V. V., Hovinga, R. M., & Wiesner, M. R. (2002). Constant Transmembrane Pressure vs.
573 Constant Permeate Flux: Effect of Particle Size on Crossflow Membrane Filtration.
574 *Environmental Engineering Science*, 19(6), 343–355.
575 <https://doi.org/10.1089/109287502320963355>
- 576 Ushikubo, F. Y., Watanabe, A. P., & Viotto, L. A. (2007). Microfiltration of umbu (*Spondias tuberosa*
577 Arr. Cam.) juice. *Journal of Membrane Science*, 288(1), 61–66.
578 <https://doi.org/https://doi.org/10.1016/j.memsci.2006.11.003>
- 579 Vaillant, F., Cisse, M., Chaverri, M., Perez, A., Dornier, M., Viquez, F., & Dhuique-Mayer, C. (2005).
580 Clarification and concentration of melon juice using membrane processes. *Innovative Food*
581 *Science & Emerging Technologies*, 6(2), 213–220.
582 <https://doi.org/https://doi.org/10.1016/j.ifset.2004.11.004>
- 583 Vaillant, F., Pérez, A. M., Acosta, O., & Dornier, M. (2008). Turbidity of pulpy fruit juice: A key factor
584 for predicting cross-flow microfiltration performance. *Journal of Membrane Science*, 325(1),
585 404–412. <https://doi.org/https://doi.org/10.1016/j.memsci.2008.08.003>
- 586 Wang, B.-J., Wei, T.-C., & Yu, Z.-R. (2005). Effect of operating temperature on component distribution
587 of West Indian cherry juice in a microfiltration system. *LWT - Food Science and Technology*,
588 38(6), 683–689. <https://doi.org/https://doi.org/10.1016/j.lwt.2004.09.002>
- 589

590 **TABLES**

591

592 Table 1: Composition of the initial cashew apple extracts obtained by pressing, coupled with
 593 or without enzyme liquefaction, and used as raw materials for crossflow microfiltration
 594 experiments (average value and standard deviation evaluated with 3 repetitions). TSS: total
 595 soluble solids; SIS: suspended insoluble solids; DM: dry matter; C: carotenoid content; p:
 596 carotenoid purity.

	TSS (g·kg⁻¹)	SIS (g·kg⁻¹)	DM (g·kg⁻¹)	C (mg·kg⁻¹)	p (mg·kg⁻¹)
Without enzyme	52 (1)	12.7 (0.1)	64.7 (1.1)	2.9 (0.1)	45 (2)
With enzyme	52 (1)	13.0 (0.2)	65.0 (1.2)	3.8 (0.1)	58 (3)

597

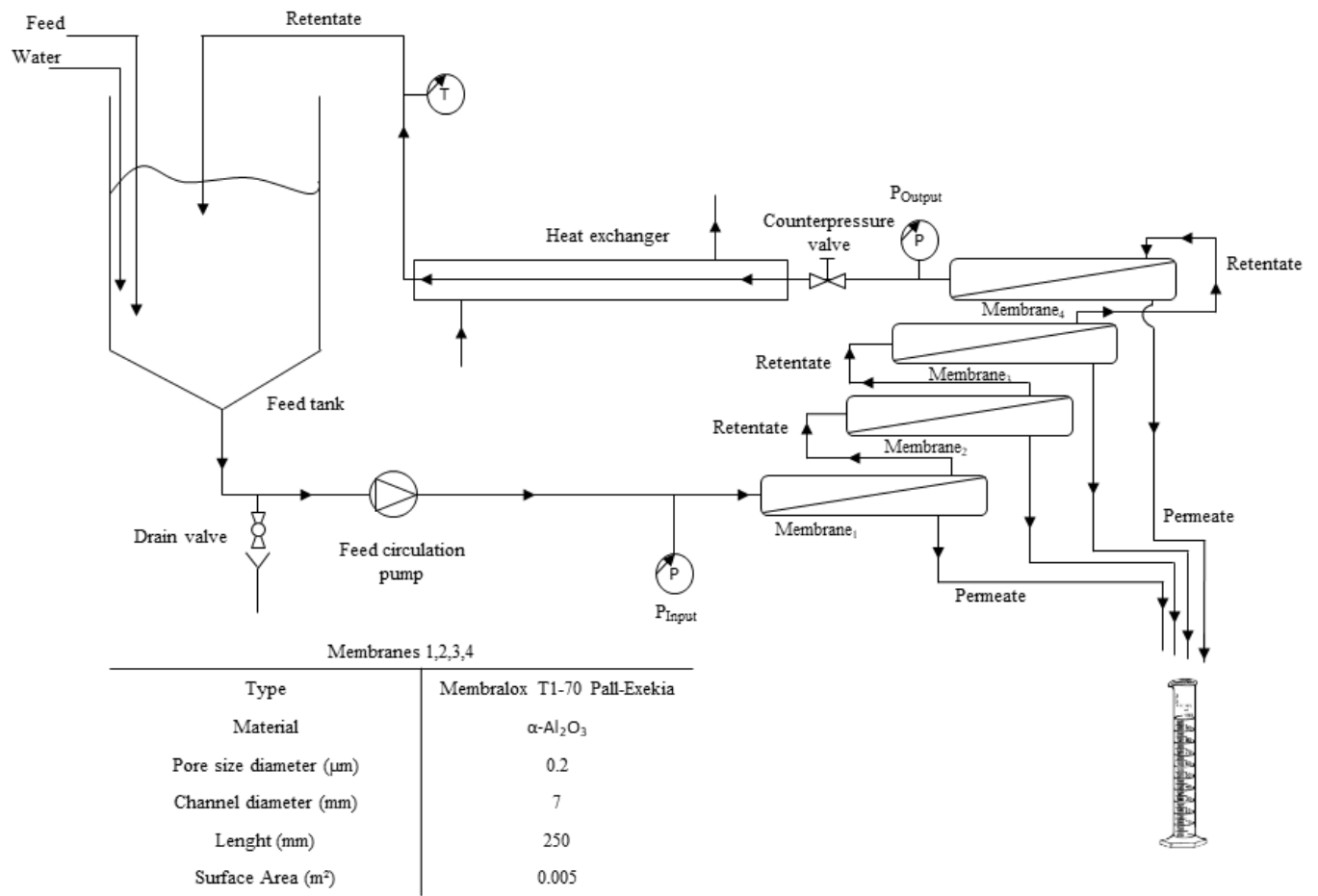
598 Table 2: Experimental (Exp.) and calculated (Calc.) composition of the concentrates obtained
 599 by microfiltration with and without enzyme liquefaction (average value and standard
 600 deviation evaluated with 3 repetitions). VRR: volume reduction ratio; DVR: diavolume ratio;
 601 TSS: total soluble solids; SIS: suspended insoluble solids; DM: dry matter; C: carotenoid

Initial extract	VRR	DVR		TSS (g·kg⁻¹)	SIS (g·kg⁻¹)	DM (g·kg⁻¹)	C (mg·kg⁻¹)	p (mg·kg⁻¹)	PF
Without enzyme	17.8	3.81	Exp.	4 (1)	227.0 (0.6)	231.0 (1.6)	54 (2)	234 (10)	5.2 (0.5)
			Calc.	1	226.1	227.1	52	228	5.1
With enzyme	19.1	3.13	Exp.	2 (1)	248.4 (1.5)	250.4 (2.5)	73 (3)	292 (15)	5.0 (0.5)
			Calc.	1	248.3	249.3	73	290	5.0

602 content; p: carotenoid purity.

603

604 **FIGURES**



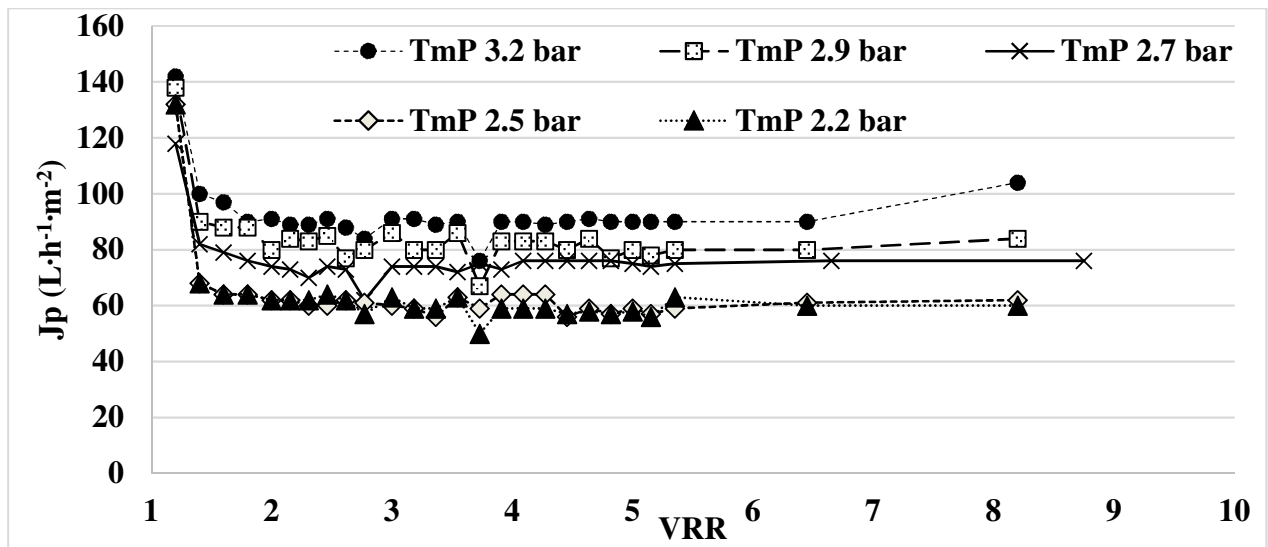
605

606 Figure 1 : Diagram of the microfiltration device and membrane characteristics

607

608

609



610

611 Figure 2: Permeate flux (J_p) vs. volume reduction ratio (VRR) during the concentration step
612 by crossflow microfiltration of the cashew apple fiber extract without enzyme liquefaction at
613 5 transmembrane pressures (TmP).

614

615

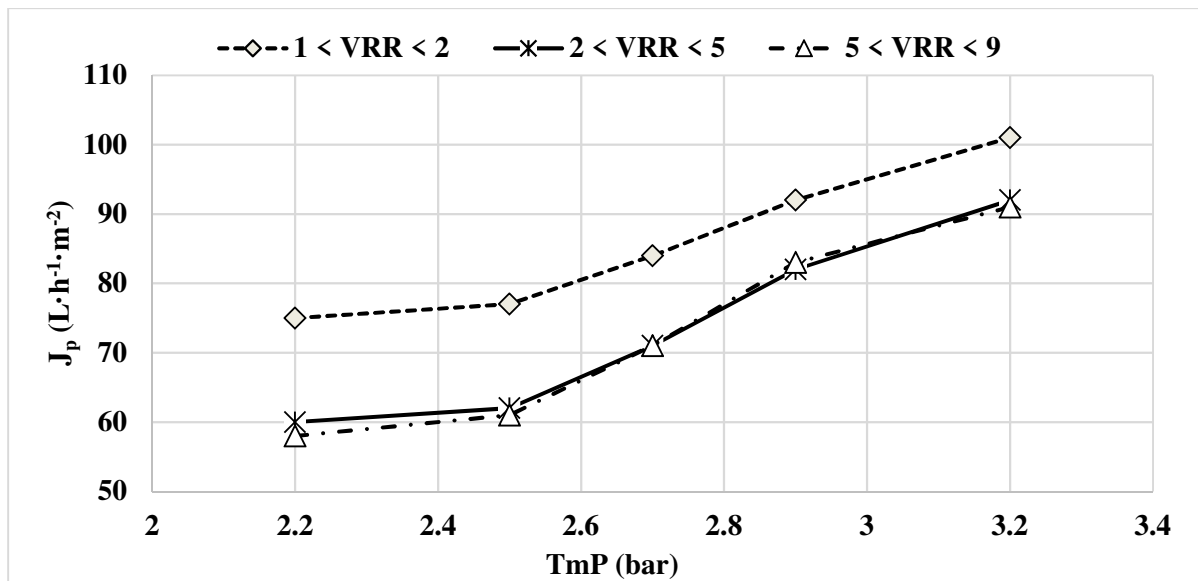
616

617

618

619

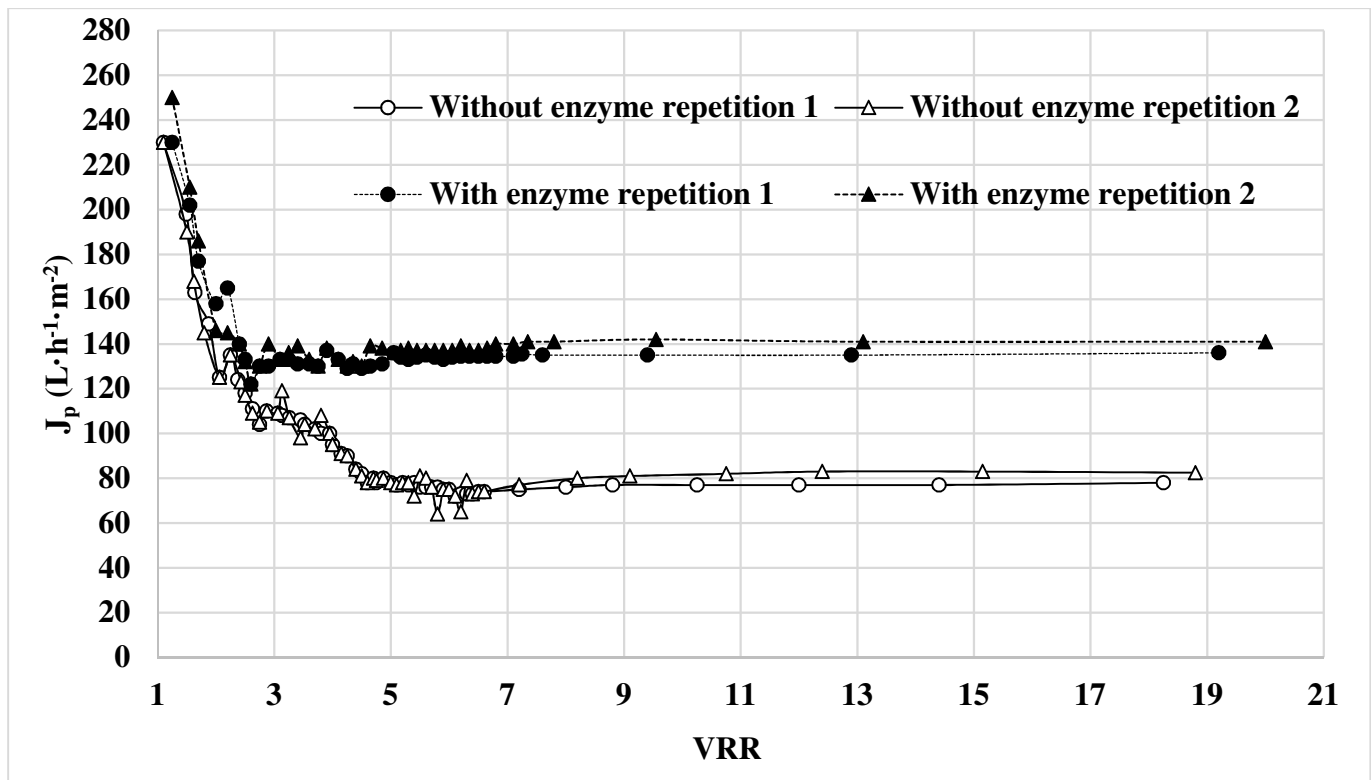
620



621

622 Figure 3: Average permeate flux (J_p) vs. transmembrane pressure (TmP) for different intervals
 623 of volume reduction ratio (VRR) during the concentration step by microfiltration of the
 624 cashew apple fiber extract without enzyme liquefaction.

625

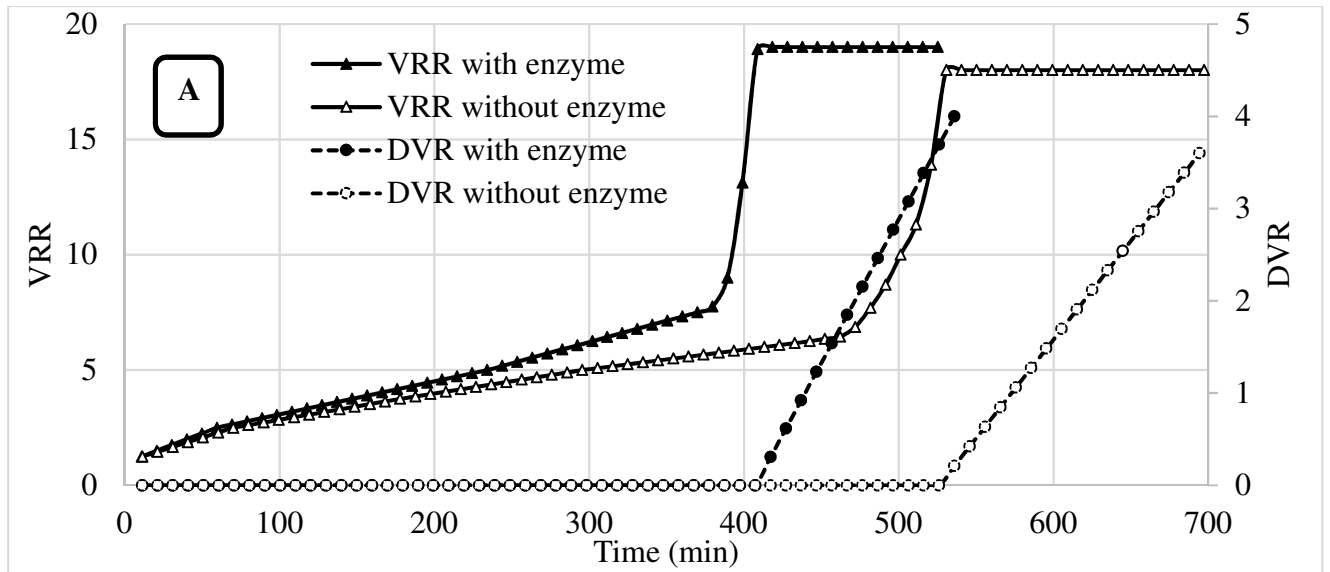


626

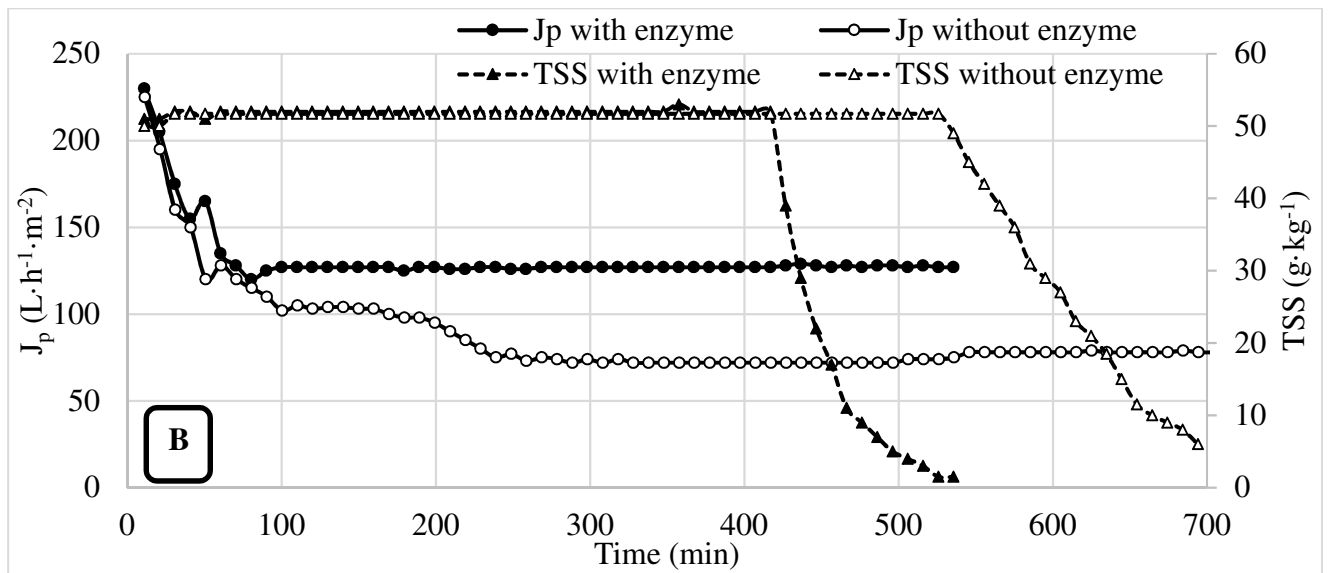
627 Figure 4: Permeate flux (J_p) vs. volume reduction ratio (VRR) during the concentration by
 628 microfiltration of cashew apple extracts with and without enzyme liquefaction (TMP = 3.2
 629 bar).

630

631



632

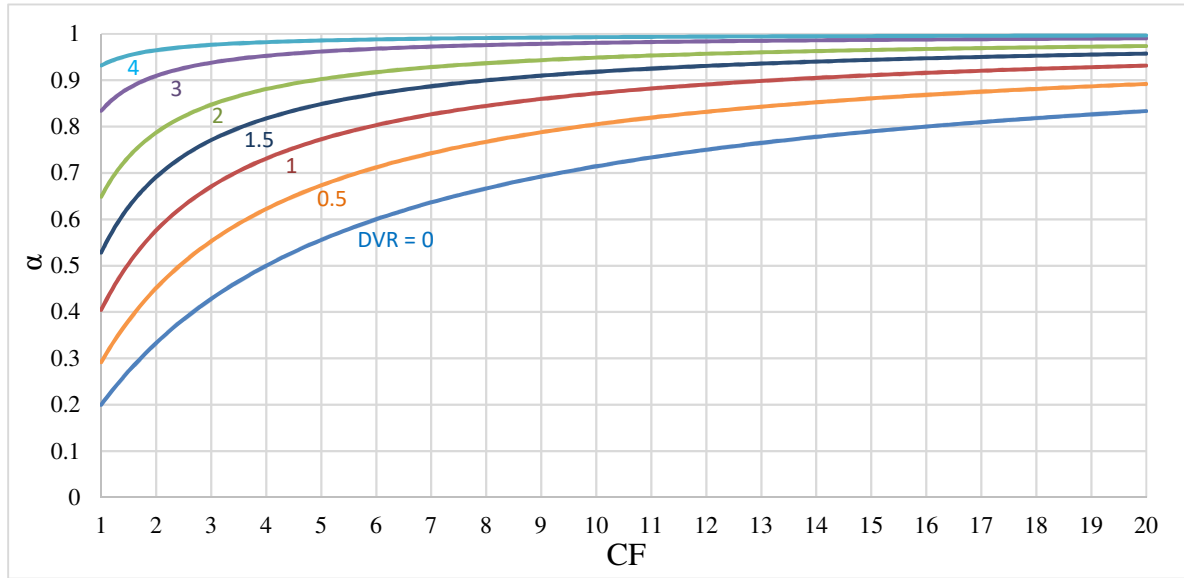


633

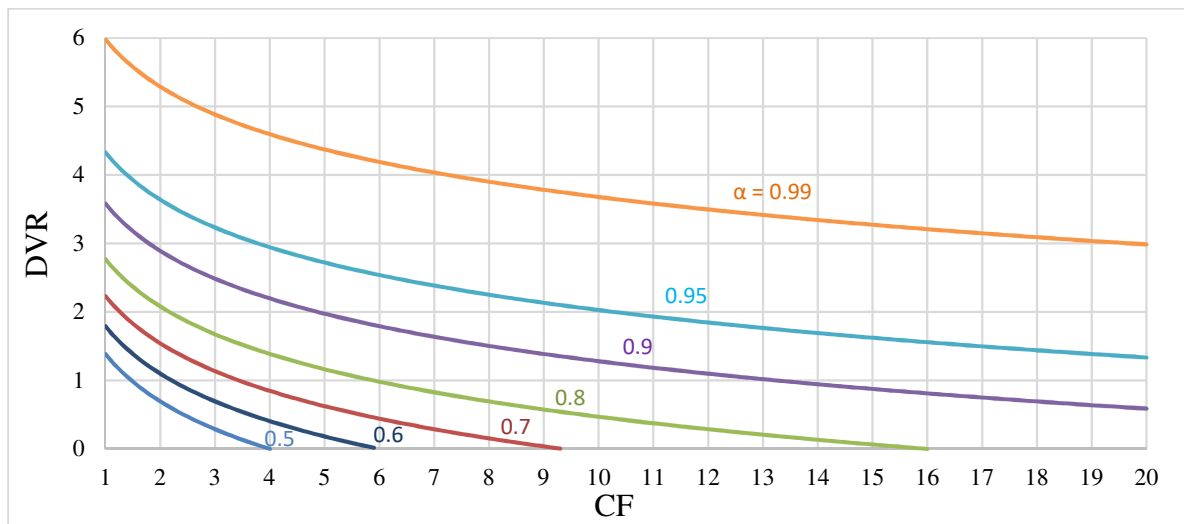
634 Figure 5: Evolution of **A**- volume reduction ratio (VRR) and diavolume ratio (DVR), and **B**-
 635 permeate flux (J_p) and total soluble solids in the concentrate (TSS) versus time during the
 636 concentration and the purification by microfiltration and diafiltration of the cashew apple
 637 extracts with and without enzyme liquefaction ($T_{mP} = 3.2$ bar).

638

639



640

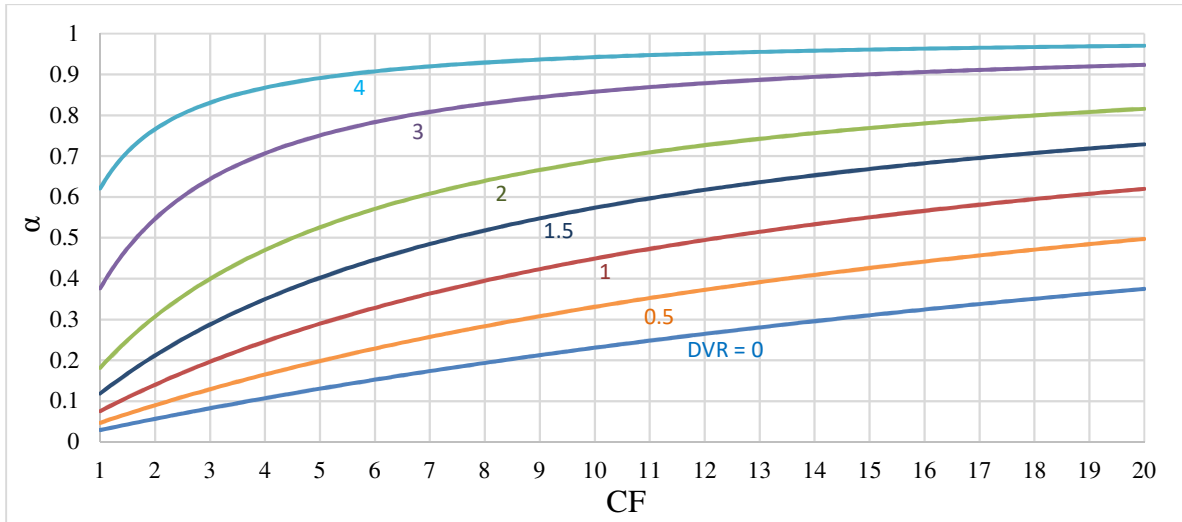


641

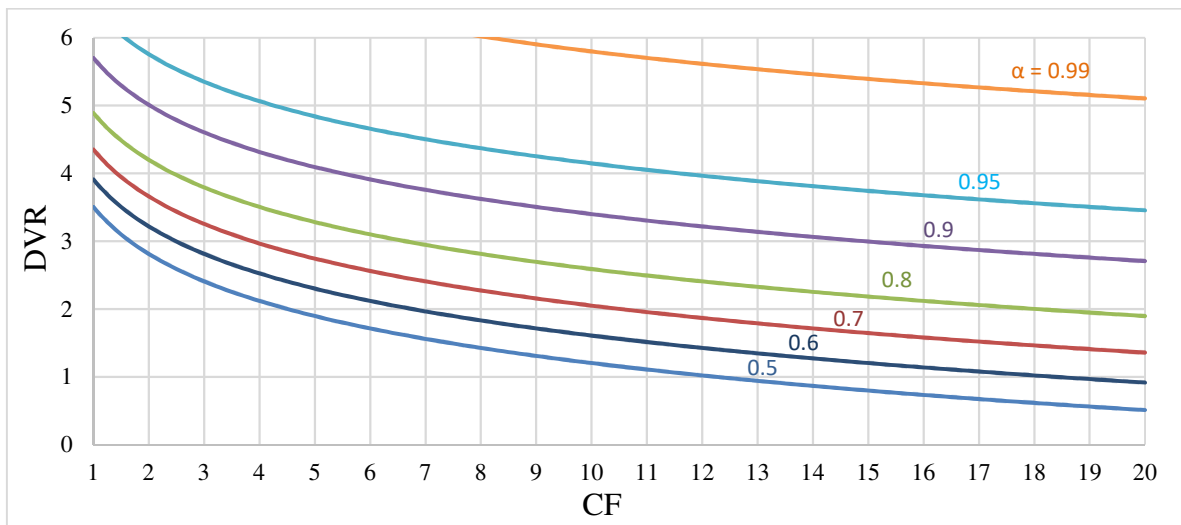
642 Figure 6: Predicted charts from the model, plotting the purification rate of carotenoids (α) that is
643 achievable for different diavolume ratios (DVR) and the DVR that is required to reach different α , as
644 a function of the concentration factor (CF), for a cashew apple fiber extract with an initial total soluble
645 and suspended insoluble solids ratio **TSS₀/SIS₀ of 4**.

646

647



648



649

650 Figure 7: Predicted charts from the model, plotting the purification rate of carotenoids (α) that is
 651 achievable for different diavolume ratios (DVR) and the DVR that is required to reach different α , as
 652 a function of the concentration factor (CF), for a citrus juice with an initial total soluble and suspended
 653 insoluble solids ratio TSS_0/SIS_0 of 33.

654

655

656